Duality of Channel Encoding and Decoding - Part I: Rate-1 Binary Convolutional Codes

Yonghui Li, *Senior Member, IEEE,* Qimin You,

Soung C. Liew, *Fellow, IEEE,* and Branka Vucetic, *Fellow, IEEE*

Abstract

In this paper, we revisit the forward, backward and bidirectional Bahl-Cocke-Jelinek-Raviv (BCJR) soft-input soft-output (SISO) maximum a posteriori probability (MAP) decoding process of rate-1 binary convolutional codes. From this we establish some interesting explicit relationships between encoding and decoding of rate-1 convolutional codes. We observe that the forward and backward BCJR SISO MAP decoders can be simply represented by their dual SISO channel encoders using shift registers in the complex number field. Similarly, the bidirectional MAP decoding can be implemented by linearly combining the shift register contents of the dual SISO encoders of the respective forward and backward decoders. The dual encoder structures for various recursive and non-recursive rate-1 convolutional codes are derived.

Index Terms

Convolutional codes, BCJR algorithm, MAP decoding, Encoding and decoding duality, Dual encoder, Bidirectional MAP decoding

I. INTRODUCTION

Convolutional codes were first introduced by Elias more than 50 years ago [1]. They have been widely used in various modern communications systems, such as space and satellite com-

munications, cellular mobile, and digital video broadcasting. Its popularity stems from its simple encoder structure, which can be implemented by shift registers.

The main complexity associated with systems using convolutional coding is situated in the decoder. Decoding essentially consists of finding an optimal path in a trellis based graph. Various decoding algorithms have been developed to achieve the optimal decoding performance in the most efficient manner. The Viterbi algorithm (VA) has been known as a maximum-likehood (ML) decoding method, which minimizes the sequence error rate [2-4]. It exhaustively searches all states of the trellis over a fixed length window and finds a most likely information sequence. In the standard VA, the decoder produces hard-decision outputs, which are the estimates of transmitted binary information symbols. In [5, 8], the VA is modified to deliver not only the most-likely binary signal sequence, but also the soft output containing the a posteriori probabilities (APPs) of the transmitted binary symbols. The soft-output VA (SOVA) is especially useful when decoding concatenated codes, such as turbo codes, as it provides soft input for the next decoding stage and thus improved performance.

There exists another class of non-linear decoding algorithms, called maximum a posteriori probability (MAP) decoding. It was first proposed by Bahl, Cocke, Jelinek and Raviv (BCJR) in 1974 [6]. It performs symbol by symbol decoding and uses the symbol error rate as the optimization criterion. Both the input and output of the decoder are soft information signals. Compared to the VA, the soft-input-soft-output (SISO) MAP can provide the optimal symbol-by-symbol APP, and thus can fully exploit the full benefits of soft-decision decoding in iterative decoding process of concatenated codes.

The BCJR MAP decoding is a bi-directional decoding process, consisting of a forward and a backward recursion process, which dominates the main complexity of a decoder. In each direction, the decoder infers the probabilities of current states and information symbols based on the probabilities of the previous states in the forward and backward trellis, the received signal, the channel state and the a priori probabilities of the transmitted signals. The complexity of forward and backward recursion exponentially increases with the constraint length of convolutional codes.

In this paper, we revisit the forward, backward and bidirectional SISO MAP decoding of rate-1 convolutional codes. We observe some interesting explicit relationship between a SISO forward/backward MAP decoder of a convolutional code and its encoder. The forward and backward decoder of a rate-1 convolutional code can actually be represented by its corresponding

dual encoder using shift registers in the complex field. This significantly reduces the original exponential computational complexity of MAP forward and backward recursion to the linear complexity. Similarly the bidirectional MAP decoding can be implemented by linearly combining the shift register contents of the dual SISO encoders of the respective forward and backward decoders. With logarithm of the soft coded symbol estimate, directly obtained from the received signals, as the input to the dual encoder, the dual encoder output produces the logarithm of the soft symbol estimates of the binary information symbols.

We found that the dual encoder structure of a code depends on whether the code is recursive or not. In our preliminary work in [9], we investigated the rate-1 recursive convolutional codes. In this paper, we will study the general rate-1 convolutional codes, including the feedback only convolutional (FBC) code, feed-forward only convolutional (FFC) code and general convolutional (GC) code. We will investigate the explicit relationship between a SISO forward/backward MAP decoder of these codes. The dual encoder structure is derived for each class of codes. In [9], the bidirectional decoding output is derived through the linear combination of forward and backward decoder outputs. These complex coefficients are found through computer search. However we only found the coefficients for some specific 4-state and 8-states codes due to the high complexity involved in the search. In this paper, we propose a simple and general combining approach to represent the bidirectional MAP decoder by linearly combining shift register contents of the dual encoders of the respective forward and backward decoders. We prove that such linear combining produces exactly the same decoding output as the bidirectional MAP decoding for any rate-1 convolutional codes.

The remainder of the paper is organized as follows. In Section II, we first briefly review the BCJR forward decoding algorithm and derive the dual encoder structures of MAP forward decoders for three classes of rate-1 convolutional codes. The dual encoder structure for backward decoding is presented in Section III. The representation of bidirectional MAP decoding by using the derived dual encoder structures of forward and backward decoding is described in Section IV. Simulation results are shown in Section V. Conclusions are drawn in Section VI.

II. Linear Representation of MAP Forward Decoding

In this section, we first revisit the BCJR forward decoding algorithm. We will focus on the decoding of a single constituent convolutional code of rate-1. Let $\mathbf{b} = (b_1, b_2, \ldots, b_K)$ be
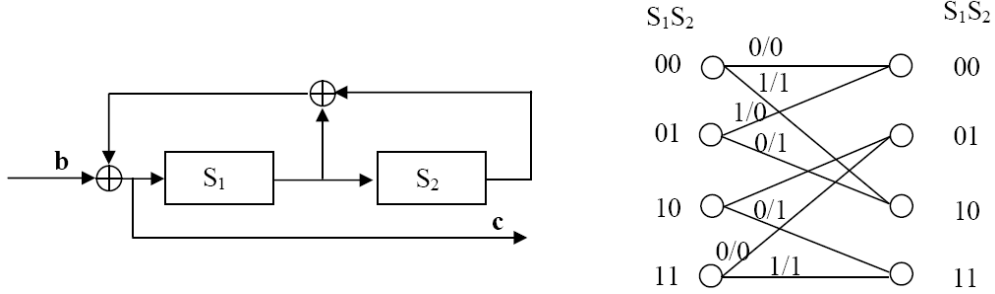
Fig. 1: The encoder and trellis of $g_{FBC}(x) = \frac{1}{x^2+x+1}$

a binary information symbol sequence to be transmitted, where K is the frame length. Let $\mathbf{c} = (c_1, c_2, \ldots, c_K)$ be the binary codeword of $\mathbf{b}$, generated by the binary code generator polynomial $\mathbf{g}$, and $\mathbf{x} = (x_1, x_2, \ldots, x_K)$ be the modulated symbol sequence of $\mathbf{c}$. For simplicity, we consider the BPSK modulation. Let $\mathbf{y} = (y_1, y_2, \ldots, y_K)$ denote the received signal sequence at the channel output.

Based on the encoder structure, we define three different classes of convolutional codes. Let $a(x) = x^n + a_{n-1}x^{n-1} + \cdots + a_1 x_1 + 1$ and $q(x) = x^n + q_{n-1}x^{n-1} + \cdots + q_1 x_1 + 1$, where n is the degree of polynomials $a(x)$ and $g(x)$. We define a convolutional code, generated by $g_{FBC}(x) = 1/q(x)$, as a feedback-only convolutional (FBC) code, a code generated by $g_{FFC}(x) = a(x)$ as a feed-forward only convolutional (FFC) code, and a code generated by $g_{GC}(x) = a(x)/g(x)$, as a general convolutional (GC) code. We will investigate the forward decoding process of these three classes of convolutional codes.

A. Forward decoding of a FBC code

In this subsection, we first investigate the forward decoding of an FBC code. To gain better insight into the decoding process, let us first look at the following example.

Example 1: We consider a FBC code with the generator polynomial of $g_{FBC}(x) = \frac{1}{x^2+x+1}$, for which the encoder and trellis diagram are shown in Fig. 1. In the trellis diagram, the state is labeled as $S_1 S_2$, where S_i, $i = 1, 2$ is the value of the i-th encoder shift register content. Each branch in the trellis is labeled as x/y where x and y denote the encoder input and output, respectively.

Let $p_{c_k}(l) = p(c_k = l|y_k)$, $l = 0, 1$, denote the a posteriori probabilities (APP) of the encoded

symbol $c_k = l$, given the received signal y_k, where c_k is the transmitted binary coded symbol at time k. Let us further denote $\mathbf{P}_c = \{(p_{c_1}(0), p_{c_1}(1)), \cdots, (p_{c_k}(0), p_{c_k}(1)), \cdots, (p_{c_K}(0), p_{c_K}(1))\}$. Now let us follow the BCJR forward decoding algorithm to use $\mathbf{P}_c$ to calculate the APPs of binary information symbols b_k. Let $p_{b_k}(w) = p(b_k = w|\mathbf{y})$ represent the probability of information symbol $b_k = w$, w=0, 1, given the received signals $\mathbf{y} = \{y_1, \cdots, y_k, \cdots, y_K\}$. It can be calculated in the following recursive way [6]

$$p_{b_k}(w) \quad = \quad p(b_k = w|\mathbf{y}) = \sum_{(m', m) \in U(b(k)=w)} \alpha_{k-1}(m')\gamma_k(m'm) \tag{1}$$

$$= \sum_{(m', m) \in U(b(k)=w)} \alpha_{k-1}(m')p_{c_k}(c_k(m', m))$$

$$\alpha_k(m) = \sum_{m'} \alpha_{k-1}(m')\gamma_k(m'm) = \sum_{m'} \alpha_{k-1}(m')p_{c_k}(c_k(m', m)), \tag{2}$$

where $U(b(k) = w)$ is the set of trellis branches from the state m' at time k-1 to the state m at time k, that are caused by the input binary symbol $b(k) = w$, and $c_k(m', m)$ represents the encoder output of the corresponding trellis branch.

Let $m = 0, 1, 2, 3$ represent the states of $S_1 S_2 = 00, 01, 10, 11$ at time k, and $\hat{\mathbf{x}}_{\mathbf{c}} = (\hat{x}_{c_1}, \cdots, \hat{x}_{c_K})$ and $\hat{\mathbf{x}}_{\mathbf{b}} = (\hat{x}_{b_1}, \cdots, \hat{x}_{b_K})$ denote the soft symbol estimate sequence of codeword $\mathbf{c}$ and information sequence $\mathbf{b}$, respectively. We assume that 0 and 1 are modulated into symbol 1 and -1. Then the soft symbol estimates $\hat{x}_{c_k}$ and $\hat{x}_{b_k}$, which represent the probabilistic average of estimates of symbols x_{c_k} and x_{b_k} given $\mathbf{y}$, can be calculated as

$$\hat{x}_{c_k} = E(x_{c_k}|y_k) = p_{c_k}(0) - p_{c_k}(1) \tag{3}$$

$$\hat{x}_{b_k} = E(x_{b_k}|\mathbf{y}) = p_{b_k}(0) - p_{b_k}(1). \tag{4}$$

Then by using Eqs. (1) and (2) alternatively in Example 1, we can get

(1) at time $k = 0$,

$\alpha_0(0) = 1$; $\alpha_0(1) = 0$; $\alpha_0(2) = 0$; $\alpha_0(3) = 0$;

$p_{b_0}(0) = 1$; $p_{b_0}(1) = 0$;

(2) at time $k = 1$, the received signal is $y(1)$, and the input to the decoder is the APPs of c_1, given by $p_{c_1}(0)$ and $p_{c_1}(1)$, respectively. Then we have

$\alpha_1(0) = p_{c_1}(0)$; $\alpha_1(1) = 0$; $\alpha_1(2) = p_{c_1}(1)$; $\alpha_1(3) = 0$;

$p_{b_1}(0) = p_{c_1}(0)$; $p_{b_1}(1) = p_{c_1}(1)$;

and

$$\hat{x}_{b_1} = p_{b_1}(0) - p_{b_1}(1) = p_{c_1}(0) - p_{c_1}(1) = \boxed{\hat{x}_{c_1}}$$

(3) at time $k = 2$, the input to the decoder is the APPs of c_2, $p_{c_2}(0)$ and $p_{c_2}(1)$. We have

$$\alpha_2(0) = p_{c_2}(0)p_{c_1}(0); \ \alpha_2(1) = p_{c_2}(0)p_{c_1}(1); \ \alpha_2(2) = p_{c_2}(1)p_{c_1}(0); \ \alpha_2(3) = p_{c_2}(1)p_{c_1}(1);$$

$$p_{b_2}(0) = p_{c_2}(0)\alpha_1(0) + p_{c_2}(1)\alpha_1(2); \ p_{b_2}(1) = p_{c_2}(1)\alpha_1(0) + p_{c_2}(0)\alpha_1(2);$$

and

$$\hat{x}_{b_2} = p_{b_2}(0) - p_{b_2}(1) = (p_{c_2}(0) - p_{c_2}(1))(p_{c_1}(0) - p_{c_1}(1)) = \boxed{\hat{x}_{c_2}\hat{x}_{c_1}}$$

(4) At time 3, we have

$$\alpha_3(0) = p_{c_3}(0)p_{c_2}(0); \ \alpha_3(1) = p_{c_3}(0)p_{c_2}(1); \ \alpha_3(2) = p_{c_3}(1)p_{c_2}(0); \ \alpha_3(3) = p_{c_3}(1)p_{c_2}(1);$$

$$p_{b_3}(0) = p_{c_3}(0)\alpha_2(0) + p_{c_3}(1)\alpha_2(1) + p_{c_3}(1)\alpha_2(2) + p_{c_3}(0)\alpha_2(3);$$

$$p_{b_3}(1) = p_{c_3}(1)\alpha_2(0) + p_{c_3}(0)\alpha_2(1) + p_{c_3}(0)\alpha_2(2) + p_{c_3}(1)\alpha_2(3);$$

and

$$\hat{x}_{b_3} = p_{b_3}(0) - p_{b_3}(1) = (p_{c_3}(0) - p_{c_3}(1))(p_{c_2}(0) - p_{c_2}(1))(p_{c_1}(0) - p_{c_1}(1)) = \boxed{\hat{x}_{c_3}\hat{x}_{c_2}\hat{x}_{c_1}}$$

(5)Similarly we can have for any $k >= 2$, we have

$$\alpha_k(0) = p_{c_k}(0)p_{c_{k-1}}(0); \ \alpha_k(1) = p_{c_k}(0)p_{c_{k-1}}(1); \ \alpha_k(2) = p_{c_k}(1)p_{c_{k-1}}(0); \ \alpha_k(3) = p_{c_k}(1)p_{c_{k-1}}(1);$$

$$p_{b_k}(0) = p_{c_k}(0)\alpha_{k-1}(0) + p_{c_k}(1)\alpha_{k-1}(1) + p_{c_k}(1)\alpha_{k-1}(2) + p_{c_k}(0)\alpha_{k-1}(3);$$

$$p_{b_k}(1) = p_{c_k}(1)\alpha_{k-1}(0) + p_{c_k}(0)\alpha_{k-1}(1) + p_{c_k}(0)\alpha_{k-1}(2) + p_{c_k}(1)\alpha_{k-1}(3);$$

and

$$\hat{x}_{b_k} = p_{b_k}(0) - p_{b_k}(1) = (p_{c_k}(0) - p_{c_k}(1))(\alpha_{k-1}(0) + \alpha_{k-1}(3) - \alpha_{k-1}(1) - \alpha_{k-1}(2))$$

$$= \boxed{\hat{x}_{c_k}\hat{x}_{c_{k-1}}\hat{x}_{c_{k-2}}}$$

where

$$(\alpha_{k-1}(0) + \alpha_{k-1}(3) - \alpha_{k-1}(1) - \alpha_{k-1}(2)) = p_{c_{k-1}}(0)p_{c_{k-2}}(0) + p_{c_{k-1}}(1)p_{c_{k-2}}(1) - p_{c_{k-1}}(0)p_{c_{k-2}}(1) - p_{c_{k-1}}(1)p_{c_{k-2}}(0) = \hat{x}_{c_{k-1}}\hat{x}_{c_{k-2}}.$$

Therefore, the decoder input and its output soft symbol estimates, $\hat{x}_{c_k}$ and $\hat{x}_{b_k}$, for the code, generated by $g_{FBC}(x) = \frac{1}{x^2+x+1}$, have the following relationship

$$\hat{x}_{b_k} = \hat{x}_{c_k}\hat{x}_{c_{k-1}}\hat{x}_{c_{k-2}}. \tag{5}$$

By taking the natural logarithm of both sides of the above equation, we get

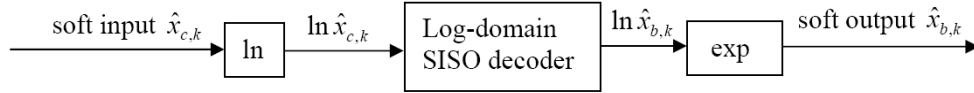$$ln\hat{x}_{b_k} = ln\hat{x}_{c_k} + ln\hat{x}_{c_{k-1}} + ln\hat{x}_{c_{k-2}}. \tag{6}$$

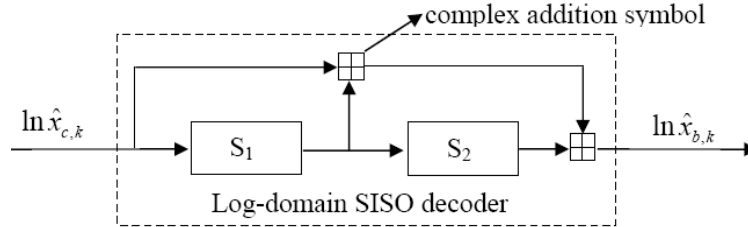Fig. 2: The relationship of a SISO decoder and its Log-domain SISO decoder

Fig. 3: The Log-domain SISO forward decoder implemented by using its dual convolutional encoder

We define the decoder with the input and output being the logarithm of the soft symbol estimates (SSE) of the coded symbols and SSEs of the information symbols, as the Log-domain soft-input-soft-output (SISO) decoder. As shown in Fig. 2, the SISO decoder can be implemented by adding a logarithm module and an exponential module at the front and rear end of the log-domain SISO decoder, respectively.

Based on Eq. 6, log-domain SISO forward decoding of the code $g_{FBC}(x) = \frac{1}{x^2+x+1}$ can be implemented by using the convolutional encoder, generated by the generator polynomial $1/g_{FBC}(x) = x^2 + x + 1$, as shown in Fig. 3. Here the addition operation in the encoder is not carried out in the binary field as in conventional convolutional encoders, but in the complex field.

Eq. 6 and Fig. 3 reveal an interesting explicit relationship of the binary encoder and SISO forward decoder of a rate-1 feedback only convolutional code. This can be generalized to any FBC codes as summarized in the following theorem.

Theorem 1 - Linear representation of forward decoding of a feedback only convolutional (FBC) code: For a FBC code, generated by a generator polynomial $g_{FBC}(x) = 1/q(x)$, we define its dual encoder as the encoder with the inverse generator polynomial of $g_{FBC}(x)$, given by $q_{FBC}(x) = 1/g_{FBC}(x) = q(x)$. Then the log-domain SISO forward decoding of the FBC code can be simply implemented by its dual encoder in the complex field. This property is shown
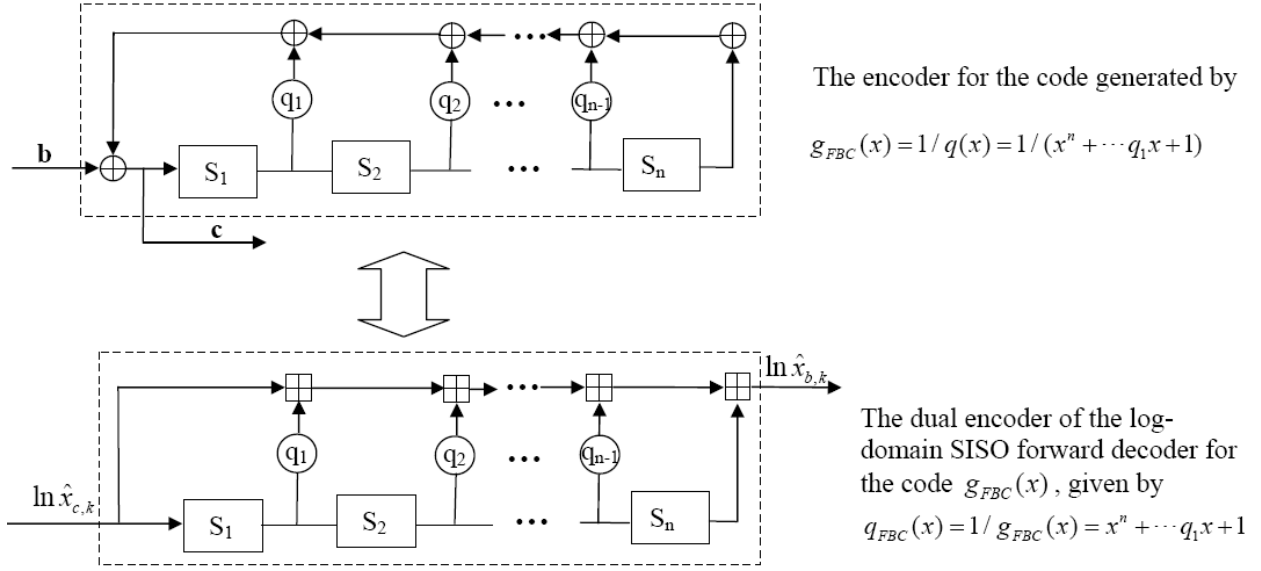
Fig. 4: Relationship of a FBC encoder and its Log-domain SISO forward decoder
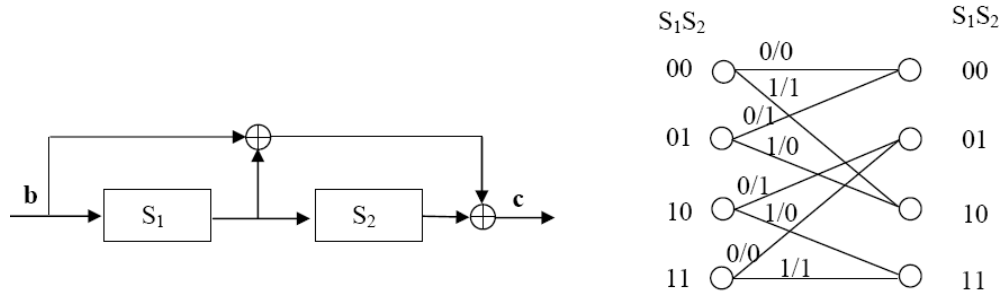

Fig. 5: The encoder and trellis of $g_{FFC}(x) = x^2 + x + 1$

in Fig. 4.

Proof: See Appendix A.

B. Forward decoding of feed-forward only convolutional (FFC) code

In this sub-section, we investigate the forward decoding of a FFC code. As will be shown in the following example, the property shown in Theorem 1 does not apply to such codes.

Example 2: We consider a FFC code with the generator polynomial of $g_{FFC}(x) = x^2 + x + 1$ for which the trellis diagram and encoder are shown in Fig. 5.

Let $ln\ddot{x}_{b_k}$ represent the output of the log-domain dual encoder, generated based on Theorem

TABLE I: Comparison of the dual encoder output calculated based on Theorem 1 $ln\ddot{x}_{b_k}$ with the actual forward MAP decoding soft output $ln\hat{x}_{b_k}$

Log soft input $ln\hat{x}_{c_k}$	Memory S_1 of the dual encoder	Memory S_2 of the dual encoder	Log soft output of the dual encoder $ln\ddot{x}_{b_k}$	Desired soft decoding output $ln\hat{x}_{b_k}$
$ln\hat{x}_{c_1}$	0	0	$ln\hat{x}_{c_1}$	$ln\hat{x}_{c_1}$
$ln\hat{x}_{c_2}$	$ln\hat{x}_{c_1}$	0	$ln\hat{x}_{c_2} + ln\hat{x}_{c_1}$	$ln\hat{x}_{c_2} + ln\hat{x}_{c_1}$
$ln\hat{x}_{c_3}$	$ln\hat{x}_{c_2} + ln\hat{x}_{c_1}$	$ln\hat{x}_{c_1}$	$ln\hat{x}_{c_3} + ln\hat{x}_{c_2} +$ $\boxed{ln\hat{x}_{c_1} + ln\hat{x}_{c_1}}$	$ln\hat{x}_{c_3} + ln\hat{x}_{c_2}$
$ln\hat{x}_{c_4}$	$ln\hat{x}_{c_3}+ln\hat{x}_{c_2}$ $+ ln\hat{x}_{c_1}+ln\hat{x}_{c_1}$	$ln\hat{x}_{c_2} + ln\hat{x}_{c_1}$	$ln\hat{x}_{c_4}+ln\hat{x}_{c_3} + ln\hat{x}_{c_1}+$ $\boxed{ln\hat{x}_{c_2}+ln\hat{x}_{c_2}+ln\hat{x}_{c_1}+ln\hat{x}_{c_1}}$	$ln\hat{x}_{c_4}+ln\hat{x}_{c_3} + ln\hat{x}_{c_1}$
$ln\hat{x}_{c_5}$	$ln\hat{x}_{c_4}+ln\hat{x}_{c_3} + ln\hat{x}_{c_1}$ $+ln\hat{x}_{c_2}+ln\hat{x}_{c_2}+ln\hat{x}_{c_1}+ln\hat{x}_{c_1}$	$ln\hat{x}_{c_3}+ln\hat{x}_{c_2}$ $+ ln\hat{x}_{c_1}+ln\hat{x}_{c_1}$	$ln\hat{x}_{c_5}+ln\hat{x}_{c_4} + ln\hat{x}_{c_2}+ln\hat{x}_{c_1} +$ $\boxed{ln\hat{x}_{c_3} +ln\hat{x}_{c_3}+ln\hat{x}_{c_2} +ln\hat{x}_{c_2}}$ $\boxed{+ln\hat{x}_{c_1}+ln\hat{x}_{c_1}+ln\hat{x}_{c_1}+ln\hat{x}_{c_1}}$	$ln\hat{x}_{c_5}+ln\hat{x}_{c_4} + ln\hat{x}_{c_2}+ln\hat{x}_{c_1}$
⋮	⋮	⋮	⋮	⋮

1, with the generator polynomial of $q_{FFC}(x) = 1/g_{FFC}(x) = 1/(x^2 + x + 1)$. Table I compares $ln\ddot{x}_{b_k}$ with the actual forward MAP decoding soft output $ln\hat{x}_{b_k}$. Their differences are highlighted in the dashed-line boxes.

From the above table, we can see that the soft outputs of the dual encoder, generated from Theorem 1, $ln\ddot{x}_{b_k}$ are different from the actual forward MAP decoding soft outputs $ln\hat{x}_{b_k}$ when $k > 2$. This is because the recursive structure of the dual encoder $q_{FFC}(x)$ and the complex field addition operation of the dual encoder. It can be observed from the above table that if the input to the dual encoder is the binary symbol and addition in the encoder is a module-2 addition, as in the conventional binary encoder, the difference terms shown in the dotted-line-boxes will become zero and the dual encoder output will be equal to the actual decoding output. However, the inputs to the dual encoder are the logarithms of the soft inputs, which are complex numbers, and the addition in the dual encoder is done in the complex-number domain, which causes the differences between $ln\ddot{x}_{b_k}$ and $ln\hat{x}_{b_k}$. We can observe from the table that the difference terms come from the common terms of the shift-register contents S_1 and S_2 in the dual encoder. If we can change structure of the dual encoder by multiplying both the numerator and denominator by a common polynomial, without changing its actual generator polynomial, such that the encoder contents do not share any common elements at any time instant, then the difference between
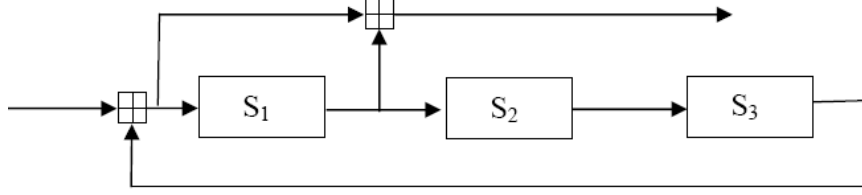
Fig. 6: The modified dual encoder of $g_{FFC}(x) = x^2 + x + 1$.

TABLE II: Comparison of modified dual encoder output $ln\ddot{x}_{b_k}$ with the actual forward MAP decoding soft output $ln\hat{x}_{b_k}$.

Log soft input $ln\hat{x}_{c_k}$	Memory S_1	Memory S_2	Memory S_3	Log soft output of the modified dual encoder $ln\ddot{x}_{b_k}$	Desired soft decoding output $ln\hat{x}_{b_k}$
$ln\hat{x}_{c_1}$	0	0	0	$ln\hat{x}_{c_1}$	$ln\hat{x}_{c_1}$
$ln\hat{x}_{c_2}$	$ln\hat{x}_{c_1}$	0	0	$ln\hat{x}_{c_2} + ln\hat{x}_{c_1}$	$ln\hat{x}_{c_2} + ln\hat{x}_{c_1}$
$ln\hat{x}_{c_3}$	$ln\hat{x}_{c_2}$	$ln\hat{x}_{c_1}$	0	$ln\hat{x}_{c_3} + ln\hat{x}_{c_2}$	$ln\hat{x}_{c_3} + ln\hat{x}_{c_2}$
$ln\hat{x}_{c_4}$	$ln\hat{x}_{c_3}$	$ln\hat{x}_{c_2}$	$ln\hat{x}_{c_1}$	$ln\hat{x}_{c_4}+ln\hat{x}_{c_3} + ln\hat{x}_{c_1}$	$ln\hat{x}_{c_4}+ln\hat{x}_{c_3} + ln\hat{x}_{c_1}$
$ln\hat{x}_{c_5}$	$ln\hat{x}_{c_4}+ln\hat{x}_{c_1}$	$ln\hat{x}_{c_3}$	$ln\hat{x}_{c_2}$	$ln\hat{x}_{c_5}+ln\hat{x}_{c_4} + ln\hat{x}_{c_2}+ln\hat{x}_{c_1}$	$ln\hat{x}_{c_5}+ln\hat{x}_{c_4} + ln\hat{x}_{c_2}+ln\hat{x}_{c_1}$
$\vdots$	$\vdots$	$\vdots$	$\vdots$	$\vdots$	$\vdots$

$ln\ddot{x}_{b_k}$ and $ln\hat{x}_{b_k}$ will disappear and the dual encoder output will be equal to the actual MAP forward decoding output.

In Example 2, if we multiply both the numerator and denominator of the dual encoder generator polynomial $q(x)$ by $(1 + x)$, then we have

$$q(x) = \frac{1+x}{g_{FFC}(x)(1+x)} = \frac{1+x}{1+x^3}. \tag{7}$$

Fig. 6 shows the encoder with the polynomial in Eq. (7).

Table II shows the outputs of the modified dual decoder and the output of the actual MAP forward decoder. We can see that the soft outputs of the modified dual encoder are exactly the same as the actual MAP forward decoding outputs.

We can prove that for any FFC codes, we can always find a modified dual decoder to implement a MAP forward decoder without changing its actual generator polynomial. This is summarized in Theorem 2.

Before we present the new theorem, we first define a *minimum complementary polynomial*.

For a given polynomial $a(x) = x^n + \cdots + a_1 x + 1$, we define the *minimum complementary polynomial* as the polynomial of the smallest degree,

$$z(x) = x^l + z_{l-1}x^{l-1} + \cdots + z_1 x + 1 \tag{8}$$

such that

$$a(x)z(x) = x^{n+l} + 1. \tag{9}$$

Since $a(x) = x^n + \cdots + a_1 x + 1$ always divides $x^{2^n-1} + 1$, the minimum complementary polynomial of $a(x)$ always exists.

Theorem 2 - Linear presentation of forward decoding of a feed-forward only convolutional (FFC) code: For a FFC code, generated by a generator polynomial $g_{FFC}(x) = a(x)$, let $z(x)$ represent its *minimum complementary polynomial* of degree l. The log-domain SISO forward decoding of the FFC code can be implemented by its dual encoder with the generator polynomial of

$$q_{FFC}(x) = \frac{z(x)}{a(x)z(x)} = \frac{z(x)}{x^{n+l}+1} = \frac{x^l + z_{l-1}x^{l-1} + \cdots + z_1 x + 1}{x^{n+l}+1}. \tag{10}$$

Proof: See Appendix B.

As it can be noted from Theorem 2, in contrast to FBC, the encoder and decoder of which can be implemented by the same number of shift registers, for the FFC the number of shift registers required in decoder will be increased compared to the encoder and the number of increased shift registers depends on the degree of its minimum complementary polynomial.

Theorem 2 can be easily extended to a general convolutional (GC) code as shown in the following corollary.

Corollary 1 - Linear presentation of forward decoding of a general convolutional (GC) code: For a GC code, generated by a generator polynomial $g_{GC}(x) = \frac{a(x)}{g(x)} = \frac{x^n+\cdots+a_1 x+1}{x^n+\cdots+g_1 x+1}$, let $z(x)$ be the degree-l minimum complementary polynomial of $a(x)$. The log-domain SISO forward decoding of the GC code can be simply implemented by its dual encoder with the generator polynomial of

$$\begin{aligned} q_{GC}(x) &= \frac{g(x)z(x)}{a(x)z(x)} = \frac{g(x)z(x)}{x^{n+l}+1} = \frac{x^{n+l} + \cdots + h_1 x + 1}{x^{n+l}+1} \\ &= 1 + \frac{h_{n+l-1}x^{n+l-1} + \cdots + h_1 x}{x^{n+l}+1}, \end{aligned} \tag{11}$$
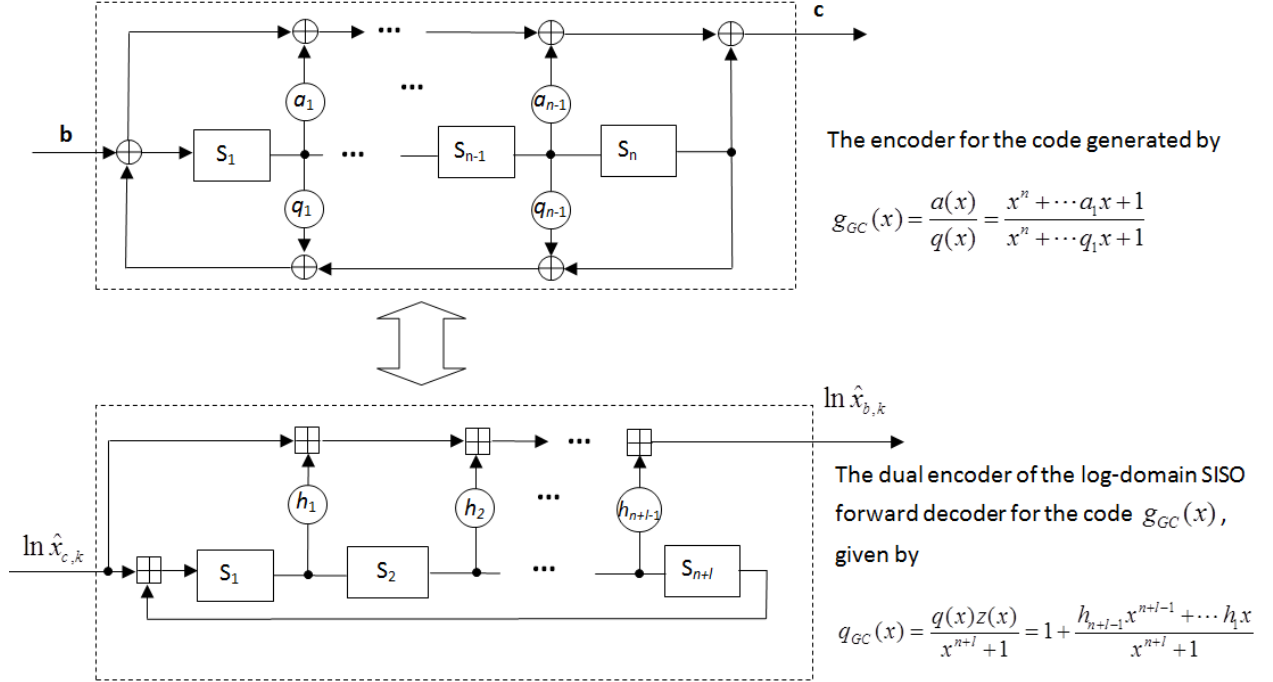
Fig. 7: The encoder and its dual encoder of forward decoding of a general convolutional (GC) code

where $g(x)z(x) = x^{n+l} + h_{n+l-1}x^{n+l-1} + \cdots + h_1 x + 1$

This relationship of a binary encoder and its dual encoder is shown in Fig. 7. Corollary 1 can be directly derived from Theorem 2, so we skip its proof here.

III. LINEAR PRESENTATION OF BACKWARD DECODING OF RATE-1 CONVOLUTIONAL CODES

In this section, we investigate the MAP backward decoding of rate-1 convolutional codes and derive its dual encoder structure. Before discussing the backward decoding, we first define a reverse memory-labeling of a general convolutional (GC) code. Given the encoder of a GC code with rational generator polynomial $g(x) = \frac{a(x)}{q(x)} = \frac{x^n + \cdots + a_1 x + 1}{x^n + \cdots + q_1 x + 1}$, if we change the labeling of the k-th shift register in the encoder from S_k to S_{n-k}, and change their respective feedforward coefficient from a_k to a_{n-k}, $k=1, 2, \ldots, n$, and feedback coefficients from b_k to b_{n-k}, $k=1, 2, \ldots, n$, we will derive an encoder with a new trellis. The resulting encoder is referred to as the *reverse memory-labeling encoder* of $g(x)$. Figs. 8(a) and 8(b) show the encoder and the reverse memory-labeling encoder of $g(x)$.
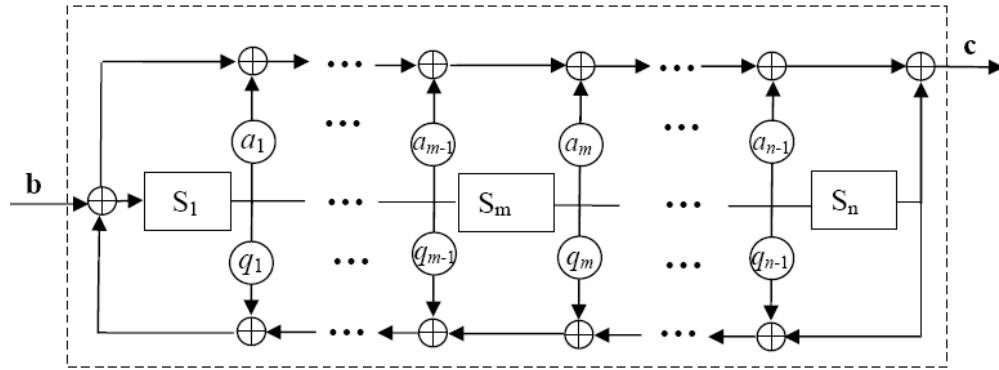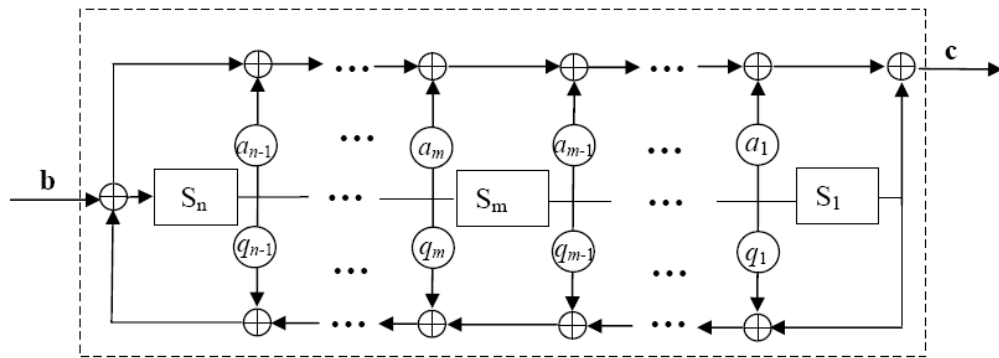
(a) The encoder of $g(x) = a(x)/q(x)$

(b) The encoder of $g(x) = a(x)/q(x)$ with reverse memory labeling

Fig. 8: An encoder with reverse memory labeling

In a MAP backward decoding, the received signals are decoded backward in a time-reverse order. That is, given the received signal sequence $\mathbf{y} = (y_1, y_2, \ldots, y_K)$, the order of signals to be decoded is from y_K, y_{K-1}, till y_1. In order to decode the received signals backward, the decoder has to follow the trellis in a reverse direction. Figs. 9(a) and 9(b) show the encoder and trellis of the code with the generator polynomial $g(x) = \frac{D^2+1}{D^2+D+1}$. Fig. 9(c) shows the backward trellis. For the decoder with the backward trellis in Fig. 9(c), the input to the decoder is at the right hand side of the decoder and its output is at the left hand side, which operates in a reverse direction of the conventional decoder. Fig. 9(d) shows the corresponding forward representation of the backward trellis, where the decoder input and output are changed to the conventional order. The forward representation of the backward trellis can be implemented by an encoder shown in Fig. 9(e). When we compare Figs. 9(a) and 9(e), it can be easily seen that the encoder in Fig. 9(a) is the encoder of code $g(x) = \frac{D^2+1}{D^2+D+1}$ and that in Fig. 9(e) is its encoder with the
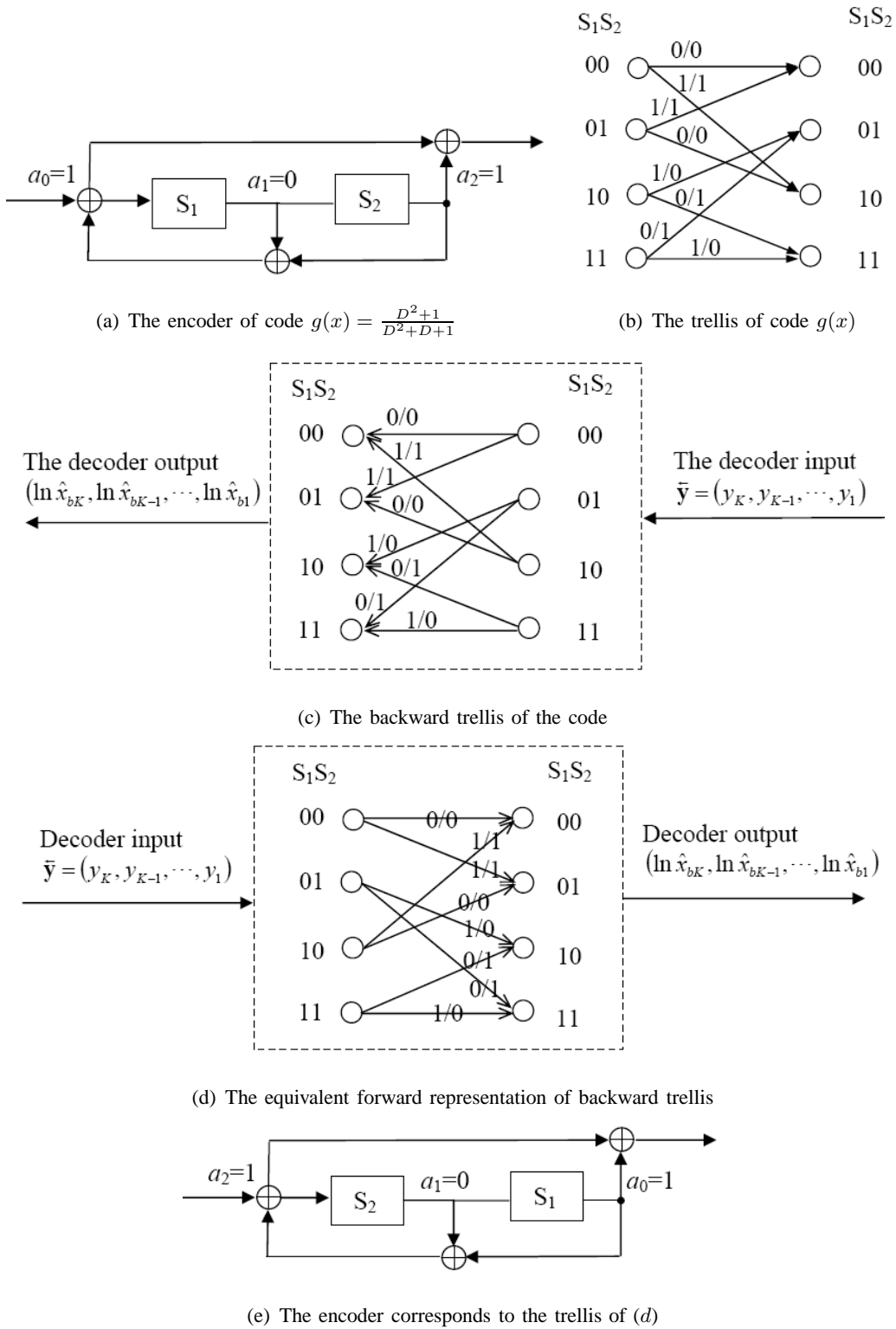
(a) The encoder of code $g(x) = \frac{D^2+1}{D^2+D+1}$

(b) The trellis of code $g(x)$

(c) The backward trellis of the code

(d) The equivalent forward representation of backward trellis

(e) The encoder corresponds to the trellis of (d)

Fig. 9: Trellis, backward trellis and their respective encoders for the code $g(x) = \frac{D^2+1}{D^2+D+1}$

reverse memory-labeling.

This relationship of the encoders for the forward and backward trellises can be extended to general rate-1 convolutional codes, as shown in the following theorem.

Theorem 3: Given an encoder with a generator polynomial $g(x) = \frac{a(x)}{q(x)} = \frac{x^n + \cdots + a_1 x + 1}{x^n + \cdots + q_1 x + 1}$, the forward representation of its backward trellis can be implemented by its *reverse memory-labeling encoder* of the same generator polynomial $g(x)$.

Proof: See Appendix C.

From Theorem 2, we know that the log-domain SISO forward decoding of a given general convolutional (GC) encoder with a generator polynomial $g(x) = \frac{a(x)}{q(x)}$ can be implemented by its dual encoder with the generator polynomial $q_{GC}(x) = \frac{q(x)z(x)}{a(x)z(x)}$, where $z(x)$ is the degree-l minimum complementary polynomial of $a(x)$. Then according to Theorem 3, the log-domain SISO backward decoding of the GC code can be implemented by the *reverse memory-labeling encoder* of $q_{GC}(x)$. By combining Theorems 2 and 3, we can obtain the linear presentation of backward decoding, which is summarized in the following Theorem.

Theorem 4 - Linear presentation of backward decoding of a general convolutional (GC) code: We consider a general convolutional encoder with a generator polynomial of $g(x) = \frac{a(x)}{q(x)} = \frac{x^n + \cdots + a_1 x + 1}{x^n + \cdots + q_1 x + 1}$. Let $z(x)$ be the degree-l minimum complementary polynomial of $a(x)$. Its log-domain SISO backward decoding can be implemented by its dual encoder with *reverse memory-labeling* and the generator polynomial of

$$
\begin{aligned}
q_{GC}(x) &= \frac{q(x)z(x)}{a(x)z(x)} = \frac{q(x)z(x)}{x^{n+l}+1} = \frac{x^{n+l} + \cdots + h_1 x + 1}{x^{n+l}+1} \\
&= 1 + \frac{h_{n+l-1}x^{n+l-1} + \cdots + h_1 x}{x^{n+l}+1}.
\end{aligned} \tag{12}
$$

This presentation is shown in Fig. 10.

From Theorem 4, we can easily derive the backward decoding presentation of a feed-forward only convolutional (FFC) code, summarized in the following Corollary.

Corollary 2 - Linear presentation of backward decoding of a feed-forward only convolutional (FFC) code: For a FFC code, generated by a generator polynomial $g_{FFC}(x) = a(x) = x^n + \ldots + a_1 x + 1$, let $z(x)$ be the degree-l minimum complementary polynomial of $a(x)$. Its log-domain SISO backward decoding can be implemented by its dual encoder with *reverse*
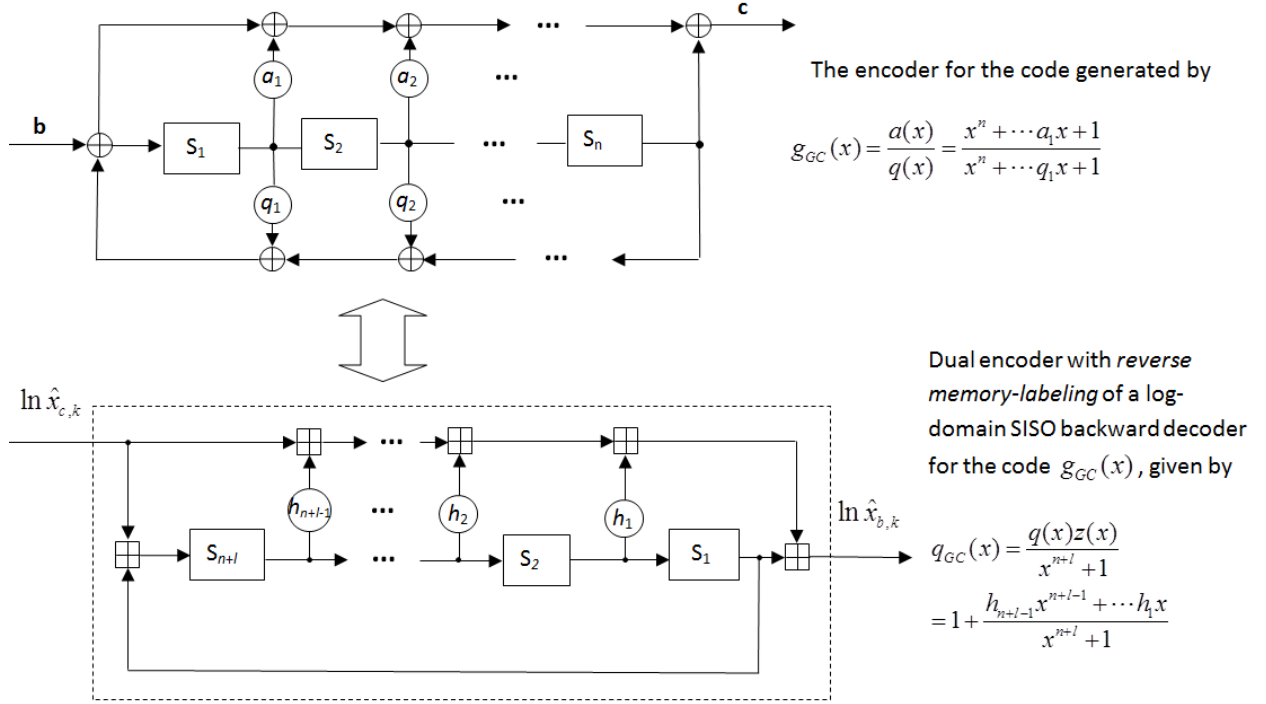
Fig. 10: The encoder and its dual encoder for backward decoding of a general convolutional code

memory-labeling and generator polynomial

$$q_{FFC}(x) = \frac{z(x)}{a(x)z(x)} = \frac{z(x)}{x^{n+l} + 1} = \frac{x^l + z_{l-1}x^{l-1} \cdots + z_1 x + 1}{x^{n+l} + 1}. \tag{13}$$

Corollary 2 can be proved in the same way as Theorem 4, so we skip the proof here.

For a feedback only convolutional (FBC) code, we can prove that backward decoding does not contribute to the MAP calculation. The BCJR MAP decoding is exactly the same as the forward decoding. This is summarized in the following Theorem.

Theorem 5 - Linear presentation of decoding of a feedback only convolutional (FBC) code: For a FBC code, generated by a generator polynomial $g_{FBC}(x) = 1/q(x)$, the MAP forward decoding is in fact equivalent to the BCJR MAP decoding. Its log-domain SISO decoder can be simply implemented by the dual encoder of the MAP forward decoding with the inverse generator polynomial of $g_{FBC}(x)$, given by $q_{FBC}(x) = 1/g_{FBC}(x)$.

Proof: See Appendix D.

From Theorem 5, we can see that the MAP decoder of a FBC code can be implemented by its dual encoder using shift registers. This significantly reduces the decoding complexity.

IV. THE REPRESENTATION OF BIDIRECTIONAL MAP DECODING

In the previous two sections, we have introduced the linear presentation of SISO MAP forward/backward decoding. Based on the derived linear presentation, in this section, we represent the bidirectional MAP decoder by linearly combining shift register contents of the dual encoders of the respective forward and backward decoders. We prove that such linear combining produces exactly the same decoding output as the bidirectional BCJR MAP decoding.

Next, let us first discuss the boundary conditions for the dual encoder. That is, how to determine the tail bits for the dual encoder such that the state of dual encoder returns to all-zero state at the end of encoding process. As we will discuss shortly, the boundary conditions are essential for shift register contents combining in the proposed decoding structure using dual encoders.

A. Boundary conditions

Let us consider a binary encoder $\bar{C}$ of memory length $n + l$, described by $q_{GC}(x) = 1 + \frac{h_1 x + \cdots + h_{n+l-1} x^{n+l-1}}{1 + x^{n+l}}$. It has the same generator polynomial as the dual encoder of a GC code C, generated by $g_{GC}(x) = \frac{a(x)}{q(x)}$. Therefore, if the input to the encoder $\bar{C}$ is a codeword $\mathbf{c} = (c_1, c_2, \cdots, c_K)$, generated by $g_{GC}(x)$, the output of the encoder $\bar{C}$ will produce the decoded binary information sequence $\mathbf{b}$. Let us define $(c_{K+1}, ..., c_{K+n+l})$ as the tail bits required to terminate the encoder $\bar{C}$ at the all-zero state. Then the tail biting convolutional encoder $\bar{C}$ has the following property.

Lemma 1: The tail bits that terminate the encoder $\bar{C}$, described by $q_{GC}(x) = 1 + \frac{h_1 x + \cdots + h_{n+l-1} x^{n+l-1}}{1 + x^{n+l}}$, at the all-zero state also terminate the encoder C, generated by $g_{GC}(x) = \frac{a(x)}{q(x)}$, at the all-zero state.

Proof: See Appendix E. ∎

Lemma 2: For a tail biting convolutional encoder $\bar{C}$, generated by $q_{GC}(x)$, and a given input sequence $(c_1, c_2, \cdots, c_K, c_{K+1}, \cdots, c_{K+n+l})$, we define its backward encoder as the encoder of the same generator polynomial with reverse-memory labeling and time-reverse input $(c_{K+n+l}, \cdots, c_{K+1}, c_K, \cdots, c_2, c_1)$. Then the tail biting encoder $\bar{C}$ and its backward encoder arrive at the same state at any time k.

Proof: See Appendix F. ∎

B. Shift register contents of the dual encoders for forward and backward decoding

In the decoding structures we introduced in the previous two sections, the input, output and shift register contents of dual encoders for forward and backward decoding are all soft symbol estimates (SSE). Let us consider a GC code, generated by $g(x) = \frac{a(x)}{q(x)}$. Let $\overrightarrow{\hat{V}}_j(k)$ and $\overleftarrow{\hat{V}}_j(k)$, $j = 1, 2, \cdots, n+l$, $k = 1, 2, \cdots, K+n+l$, represent the jth shift register content of the dual encoders for forward and backward decoding at time k, described by the polynomial $q_{GC}(x)$.

To derive the bidirectional soft decoder output, we combine the shift register contents of dual encoders for forward and backward decoding in an optimal way. Let $\overrightarrow{S}'_i(k)$ and $\overleftarrow{S}'_i(k)$, $i = 1, 2, \cdots, n+l$, denote the memory of the ith shift register at time k in the encoder $\bar{C}$ and its backward encoder. Let $P_{\overrightarrow{S}'_i(k)}(\omega)$ and $P_{\overleftarrow{S}'_i(k)}(\omega)$ denote the probability of $\overrightarrow{S}'_i(k) = \omega$ and $\overleftarrow{S}'_i(k) = \omega$ in the dual encoders of forward and backward decoding, respectively. Their corresponding LLRs are denoted by $\overrightarrow{L}_{S'_i}(k)$ and $\overleftarrow{L}_{S'_i}(k)$. Their combined LLR is denoted by $L_{S'_i}(k)$. Since $\overrightarrow{L}_{S'_i}(k)$ and $\overleftarrow{L}_{S'_i}(k)$ are obtained from the forward decoding based on the received signals from time 1 to k and that from backward decoding based on the received signals from time $K+n+l$ to $k+1$, they are independent. Furthermore, as shown in Lemma 2, for tail bitting encoder $\bar{C}$, generated by $q_{GC}(x)$, forward and backward encoders will arrive at the same state at time k. Therefore, in the optimal combining, we have

$$L_{S'_i}(k) = \overrightarrow{L}_{S'_i}(k) + \overleftarrow{L}_{S'_i}(k). \tag{14}$$

Converted into the SSE representation, (14) can be rewritten as

$$\hat{V}_j(k) = \frac{\overrightarrow{\hat{V}}_j(k) + \overleftarrow{\hat{V}}_j(k)}{1 + \overrightarrow{\hat{V}}_j(k)\overleftarrow{\hat{V}}_j(k)}. \tag{15}$$

Based on the dual encoder structure in Fig. 7b, the bidirectional soft decoder output can be obtained from the combined shift register contents as

$$\ln \hat{x}_{b_k} = \ln \hat{x}_{c_k} + \sum_{i=1}^{n+l-1} h_i \ln \hat{V}_i(k-1). \tag{16}$$

As shown in the following theorem, such combining will produce exactly the same output as the bidirectional BCJR MAP algorithm.

Theorem 6 - Shift register content combining of dual encoders of forward and backward decoding: We can represent the bidirectional MAP decoder by linearly combining shift register contents of the dual encoders for forward and backward decoding, as shown in (16). Such a combining produces exactly the same decoding output as the bidirectional BCJR MAP decoding.

Proof: See Appendix G. ∎

V. Simulation Results

In this section, we provide the simulation results. All simulations are performed for the BPSK modulation and a frame size of K=128 symbols over AWGN channels.

Figs. 11 to 16 show the bit error rate (BER) performance of various 4-state and 8-state GC and FFC codes, where the curve 'Dual encoder forward + backward' refers to the direct summation of forward and backward dual encoder outputs, and the curve 'Dual encoder shift register combined output' refers to the optimal combining of forward and backward dual encoders as shown in Theorem 6.

From figures, we can see that direct summation of forward and backward dual encoder outputs has about $1dB$ performance loss when compared to the bidirectional MAP decoding for the GC code $[5/7]_8$ at the BER of 10^{-5}. This performance loss is reduced to around $0.2dB$, $0.3dB$, and $0.4dB$ for $[7]_8$ FFC, $[17]_8$ FFC, and $[15]_8$ FFC codes, respectively and increased to more than $1dB$ for the $[15/13]_8$ GC code. However, when we apply the shift register combining approach detailed in Section IV to the forward and backward dual encoder, their performance is exactly the same as the BCJR MAP decoding. One particular point needs to be noted is that for the FFC code $[5]_8$ the direct summation of forward and backward dual encoder outputs has the same performance as the MAP decoding, so no linear combination is actually required.

VI. Conclusions

In this paper, we revisited the MAP forward and backward decoding process for the rate-1 convolutional codes. Dual encoder structures of forward and backward decoding for three different classes of rate-1 convolutional codes are derived. The input to the dual encoder is the logarithm of soft symbol estimates of the coded symbols obtained from the received signals, and the dual encoder output produces the logarithm of the soft symbol estimates of the information symbols. For the general convolutional (GC) codes, generated by a generator polynomial $g_{GC}(x) = \frac{a(x)}{q(x)}$,
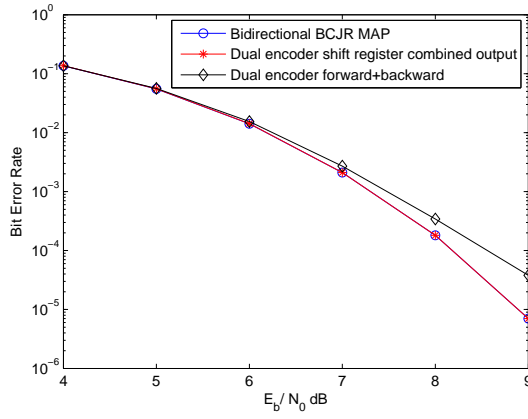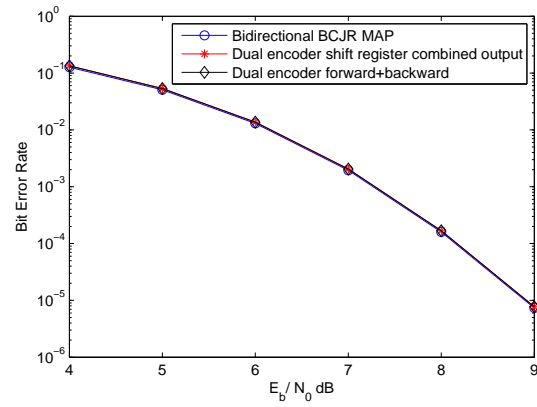
Fig. 11 BER performances of code $[5/7]_8$

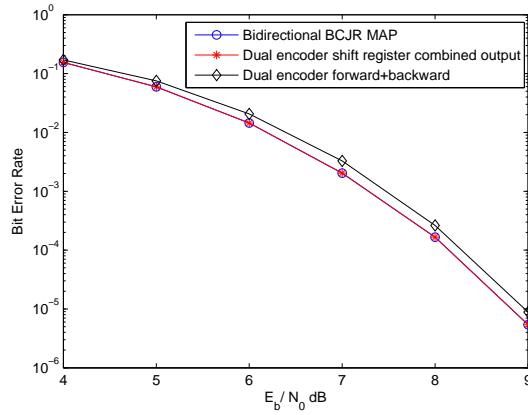Fig. 12 BER performances of code $[5]_8$

Fig. 13: BER performances of code $[7]_8$
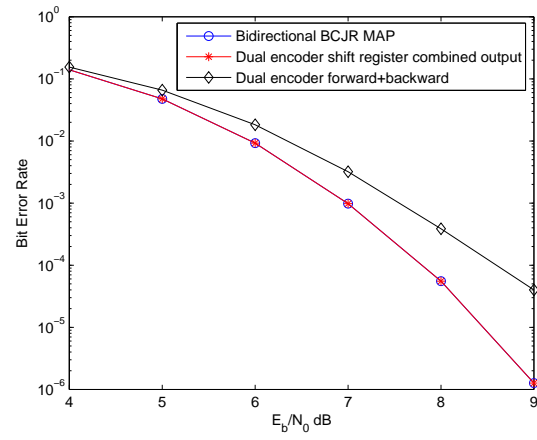

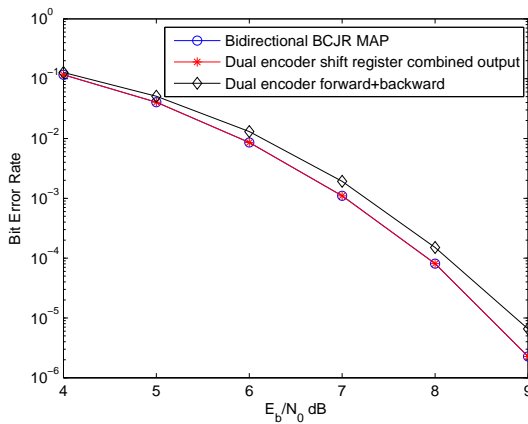Fig. 14: BER performances of code $[15/13]_8$
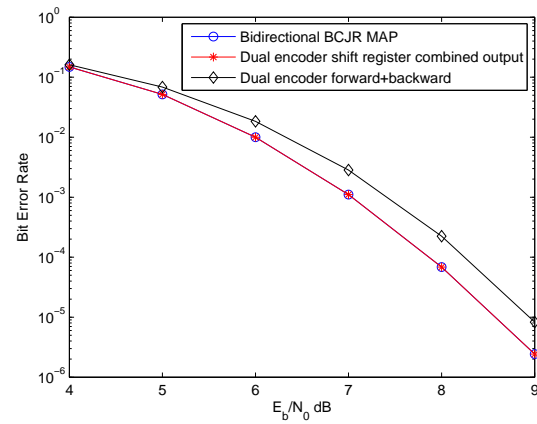

Fig. 15: BER performances of code $[17]_8$

Fig. 16: BER performances of code $[15]_8$

the forward and backward decoding can be implemented by their corresponding dual encoders, which are generated by the polynomial, $\frac{q(x)z(x)}{a(x)z(x)}$, where $z(x)$ is the *minimum complementary polynomial* of $a(x)$. The feed-forward only convolutional (FFC) code is just a special case of GC code, so it has the same dual encoder structures as the GC code. The derived linear presentation of decoder significantly reduced the the computational complexity of MAP forward and backward recursion from exponential to linear. Similarly, the bidirectional MAP decoder of GC and FFC codes can be implemented by linearly combining the shift register contents of dual encoders for the forward and backward decoding. For a feedback only convolutional (FBC) code $g_{FBC}(x) = \frac{1}{q(x)}$, the bidirectional MAP SISO decoder is equivalent to the dual encoder for the forward decoding, with the generator polynomial $q(x)$.

In this paper, we have only focused on a class of convolutional codes, named rate-1 binary code. It is significant as component codes in concatenated coding schemes, such as turbo coding. Also, the linear presentation of MAP decoding derived in this paper can also be applied to other codes and other applications. For example, the transmission of digital signals in the presence of inter-symbol interference (ISI) can also be represented by a convolutional encoding process. The channel transfer function of an ISI channel can be represented by a rate-1 convolutional encoder. Thus the linear presentation of decoding can also be applied to facilitate the MAP channel detection in ISI channels. Similarly, these properties should exist for other linear codes that are amenable to representation by a trellis diagram. We will discuss these in the next series papers.

VII. APPENDIX

A. Proof of Theorem 1

Let us consider a feedback only convolutional (FBC) code, generated by a generator polynomial

$$g_{FBC}(x) = 1/q(x) = 1/(q_n x^n + \cdots q_1 x + 1), \tag{17}$$

its encoder is shown in Fig. 4. Let $S_i(k), i = 1, \ldots, n$ represent the state of memory i at time k. Then according to Fig. 4 we have

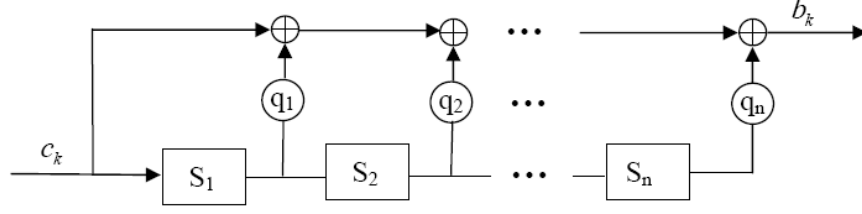$$c_k = S_1(k) = b_k \oplus \sum_{i=1}^{n} q_i S_i(k-1) \tag{18}$$

Fig. 17: Binary Decoder Structure of a FBC code generated by $g_{FBC}(x)$

$$S_p(k) = S_{p-1}(k-1), p \geq 2, \tag{19}$$

where all summations are done in GF(2).

We can rewrite the above equation as follows

$$b_k = c_k \oplus \sum_{i=1}^{n} q_i S_i(k-1) \tag{20}$$

$$S_1(k) = c_k, S_p(k) = S_{p-1}(k-1), p \geq 2 \tag{21}$$

$$S_p(k) = c_{k-p}, \tag{22}$$

where we assume that $c_k = 0$ for $k \leq 0$.

Based on the above equation, we can derive the following binary decoder structure in Fig. 17, where the input is the codeword symbol c_k and the output is b_k.

Let $P_{S_i(k)}(w)$ denote the probability of memory $S_i(k) = w$ and $\alpha_k(m)$ denote the probability of state m at time k. Let $(m_1, \cdots, m_n)$ be the n-dimensional binary representation of m and $(m'_1, \cdots, m'_n)$ be the binary representation of m'. At time k, with input c_k, the state transits from $(m'_1, \cdots, m'_n)$ to $(m_1, m_2, \cdots, m_n) = (c_k, m'_1, \cdots, m'_{n-1})$. Then we have

$$
\begin{aligned}
\alpha_k(m) &= \prod_{i=1}^{n} P_{S_i(k)}(m_i) = P(c_k = m_1) \prod_{i=2}^{n} P_{S_i(k)}(m_i) \tag{23} \\
&= P(c_k = m_1) \sum_{m'_n = 0,1} P_{S_n(k-1)}(m'_n) \prod_{i=2}^{n} P_{S_i(k)}(m_i) \\
&= \sum_{m'_n = 0,1} \left(\prod_{j=1}^{n} P_{S_j(k-1)}(m'_j) \right) P(c_k = m_1) \\
&= \sum_{m'} \alpha_{k-1}(m') \gamma_k(m', m),
\end{aligned}
$$

where $\alpha_{k-1}(m') = \prod_{j=1}^{n} P_{S_j(k-1)}(m'_j)$, $\gamma_k(m', m) = P(c_k = m_1)$ and $m'_j = m_{j+1}$, for $j = 1, 2, \ldots, n-1$.

The APP of $b_k = w$ can then be calculated as

$$
\begin{aligned}
p_{b_k}(w) &= p(b_k = w | \mathbf{y}) = \sum_{(m', m) \in U(b(k) = w)} \prod_{j=1}^{n} P_{S_j(k-1)}(m'_j) P(c_k = m_1) \qquad (24) \\[2mm]
&= \sum_{m_1, m'_1, \cdots, m'_n, \; m_1 \oplus \sum_{j=1}^{n} q_j m'_j = w} \prod_{j=1}^{n} P_{S_j(k-1)}(m'_j) P(c_k = m_1) \\[2mm]
&= \sum_{m_1, m'_1, \cdots, m'_n, \; m_1 \oplus \sum_{j=1}^{n} q_j m'_j = w} \prod_{j=1}^{n} P(c_{k-j} = m'_j) P(c_k = m_1) \\[2mm]
&= \sum_{m'_0, m'_1, \cdots, m'_n, \; \sum_{j=0}^{n} q_j m'_j = w} \prod_{j=0}^{n} P(c_{k-j} = m'_j),
\end{aligned}
$$

where $m'_0 = m_1$ and $q_0 = 1$.

Let $L(b_k)$ represent the LLR of b_k. From Eq. (24) we can easily derive

$$
L(b_k) = L\left(\sum_{j=0}^{n} q_j c_{k-j} \right). \qquad (25)
$$

Following the L-sum theory [7], the right-hand side of (25) can be expanded as

$$
L\left(\sum_{j=0}^{n} q_j c_{k-j} \right) = \ln \frac{1 + \prod_{j=0}^{n} \tanh(L\left(q_j c_{k-j} \right) / 2)}{1 - \prod_{j=0}^{n} \tanh(L\left(q_j c_{k-j} \right) / 2)}, \qquad (26)
$$

where $\tanh(x/2) = \frac{e^x - 1}{e^x + 1}$.

Then by using the following relationship between the LLR and soft symbol estimate,

$$
\hat{x}_{b_k} = \frac{e^{L(b_k)} - 1}{e^{L(b_k)} + 1} = \tanh\left(L(b(k)/2) \right), \qquad (27)
$$

$$
L(b_k) = \ln \frac{1 + \hat{x}_{b_k}}{1 - \hat{x}_{b_k}}, \qquad (28)
$$

(25) can be further written as

$$
L(b_k) = L\left(\sum_{j=0}^{n} q_j c_{k-j} \right) = \ln \frac{1 + \prod_{j=0}^{n} \hat{x}_{q_j c_{k-j}}}{1 - \prod_{j=0}^{n} \hat{x}_{q_j c_{k-j}}} = \ln \frac{1 + \prod_{j=0}^{n} \left(\hat{x}_{c_{k-j}} \right)^{q_j}}{1 - \prod_{j=0}^{n} \left(\hat{x}_{c_{k-j}} \right)^{q_j}}, \qquad (29)
$$

where $\hat{x}_{q_j c_{k-j}}$ denotes the soft symbol estimate of symbol $q_j c_{k-j}$. Obviously $\hat{x}_{q_j c_{k-j}} = 1$ when $q_j = 0$ and $\hat{x}_{q_j c_{k-j}} = \hat{x}_{c,k-j}$ when $q_j = 1$. Thus $\hat{x}_{q_j c_{k-j}} = \left(\hat{x}_{c_{k-j}} \right)^{q_j}$.

By substituting (29) into (27), we get

$$\hat{x}_{b_k} = \prod_{j=0}^{n} \left(\hat{x}_{c_{k-j}} \right)^{q_j}. \tag{30}$$

By taking the logarithm on both sides of (30), we have

$$\ln \hat{x}_{b_k} = \sum_{j=0}^{n} q_j \ln \hat{x}_{c_{k-j}}. \tag{31}$$

Therefore, the log-domain SISO forward decoding of the FBC code can be simply implemented by its dual encoder, generated by the generated polynomial $q_{FBC}(x) = 1/g_{FBC}(x) = q_n x^n + \cdots q_1 x + 1$.

This proved Theorem 1.

B. Proof of Theorem 2

Let us first examine the forward binary decoding. Based on the code generator polynomials, we can easily derive the binary decoder of codes generated by $a(x)$ and $\frac{a(x)z(x)}{z(x)} = \frac{x^{n+l}+1}{z(x)}$, as shown in Fig. 18(a) and 18(b), respectively. As can be seen from these figures, the binary decoder of each of these two codes is equivalent to the encoder generated by its respective inverse polynomial.

Let $(m_1, \cdots, m_n)$ and $(m'_1, \cdots, m'_n)$ be the n-dimensional binary representation of m and m'. Let $(u_1, \cdots, u_{n+l})$ and $\left(u'_1, \cdots, u'_{n+l} \right)$ be the $(n+l)$-dimensional binary representation of u and u'. Assume that at time k, with input c_k, the state transits from $(m'_1, \cdots, m'_n)$ to $(m_1, m_2, \cdots, m_n)$ in the binary decoder of Fig. 18(a) and transits from $(u'_1, \cdots, u'_{n+l})$ to $(u_1, \cdots, u_{n+l})$ in 18(b). For a binary input sequence $\mathbf{c} = (c_1, c_2, \cdots, c_K)$, it is well known that the polynomials $\frac{1}{a(x)}$ and $\frac{z(x)}{a(x)z(x)}$ generate the same codeword. We thus have
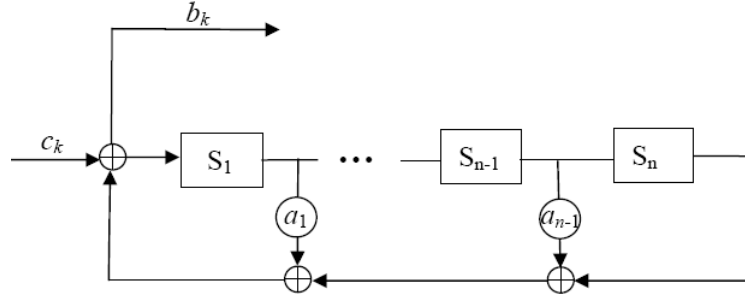
$$b_k = \sum_{i=1}^{n-1} a_i m'_i + m'_n + c_k = \sum_{j=1}^{n+l-1} z_j u'_j + u'_{n+l} + c_k, \tag{32}$$

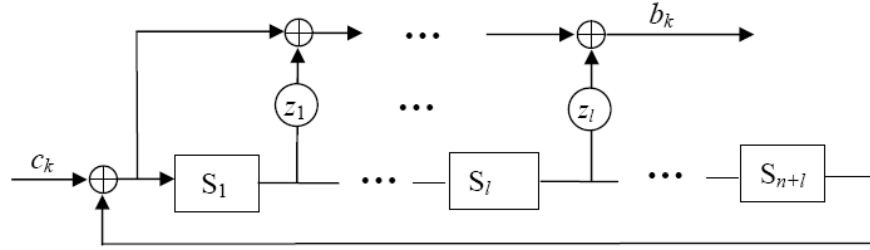$$m_j = m'_{j-1}, \ and \ u_j = u'_{j-1}, j \geq 2. \tag{33}$$

Then by following similar calculation in Appendix A, we have

$$L(b_k) = L \left(\sum_{i=1}^{n-1} a_i m'_i + m'_n + c_k \right), \tag{34}$$

(a) The binary decoder of FFC code generated by $a(x)$, which is equivalent to an encoder generated by $1/a(x)$

(b) The binary decoder of FFC code generated by $\frac{a(x)z(x)}{z(x)} = \frac{x^{n+l}+1}{z(x)}$, which is equivalent to an encoder generated by $\frac{z(x)}{a(x)z(x)} = \frac{z(x)}{x^{n+l}+1}$

Fig. 18: The binary dual encoder of a FFC code

$$L(b_k) = L\left(\sum_{j=1}^{n+l-1} z_j u'_j + u'_{n+l} + c_k \right). \tag{35}$$

When the terms in the summation of the right-hand side in (34) and (35) are statistically independent, we can use the L-sum theory to further expand these two equations. However, we can easily check that the terms m'_i, $i = 1, \cdots, n$, in (34), are not independent. Now let us prove that u'_i, $i = 1, \cdots, n + l$ are statistically independent random variables.

When $0 < k < n + l$, the state u'_i, $i = 1, \cdots, n + l$, at time k, is given by

$$u'_i = 0, k < i \text{ and } u'_i = c_{k-i}, k \geq i. \tag{36}$$

When $k > n + l$, the state u'_i, $i = 1, \cdots, n + l$, at time k, is given by

$$u'_i = \sum_{p=0}^{\lfloor k/(n+l) \rfloor} c_{k-pi}, \tag{37}$$

where $\lfloor x \rfloor$ denotes the largest integer not greater than x.

From (36) and (37), we can see that u'_i, $i = 1, \cdots, n + l$, are statistically independent random variables at any time instant k.
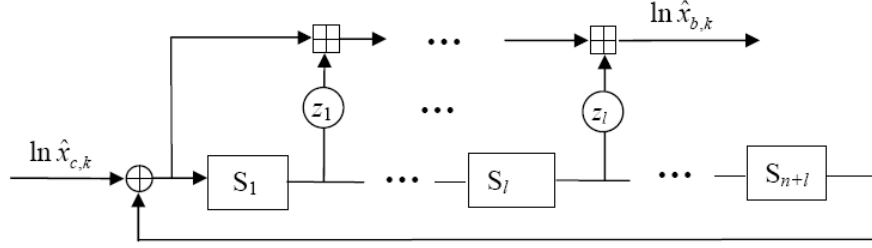
Fig. 19: The SISO decoder structure, implemented with the encoder with the generator polynomial of $q_{FFC}(x) = \frac{z(x)}{a(x)z(x)} = \frac{z(x)}{x^{n+l}+1}$

Since u'_i, $i = 1, \cdots, n + l$ are statistically independent random variables, we can use the L-sum theory [7] to expand the right-hand side of (36). By following a similar calculation as in Appendix A, we can obtain the following equation

$$\ln \hat{x}_{b_k} = \sum_{j=1}^{n+l-1} z_j \hat{x}_{u'_j} + \hat{x}_{u'_{n+l}} + \hat{x}_{c_k}, \tag{38}$$

and,

$$\hat{x}_{u_j} = \hat{x}_{u'_{j-1}}, j \geq 2, \tag{39}$$

where $\hat{x}_{b_k}$, $\hat{x}_{u_j}$, $\hat{x}_{u'_j}$ and $\hat{x}_{c_k}$ denotes the soft symbol estimate of symbol b_k, u_j, u'_j, and c_k, respectively. Based on (38) and (39), we can derive the SISO decoder structure, shown in Fig. 19, implemented with the encoder with the generator polynomial of

$$q_{FFC}(x) = \frac{z(x)}{a(x)z(x)} = \frac{z(x)}{x^{n+l}+1}. \tag{40}$$

This proves Theorem 2.

C. Proof of Theorem 3

Assume that the encoder with the generator polynomial $g(x)$ in Fig. 8(a) transits from the state $(m'_1, m'_2, \cdots, m'_n)$ at time k-1 to the state $(m_1, m_2, \cdots, m_n)$ at time k with input b_k, then we have

$$m_1 = b_k + \sum_{p=1}^{n-1} q_p m'_p + m'_n, \; m_p = m'_{p-1}, \; p \geq 2, \tag{41}$$

and the corresponding trellis output at time k is given by

$$
\begin{aligned}
c(k) &= b_k + \sum_{p=1}^{n-1} q_p m'_p + m'_n + \sum_{p=1}^{m-1} a_p m'_p + m'_m \\
&= b_k + \sum_{p=1}^{n-1} q_p m'_p + \sum_{p=1}^{m-1} a_p m'_p + m'_n + m'_m.
\end{aligned}
\tag{42}
$$

To prove Theorem 3, we now only need to prove that with input b_k its *reverse memory-labeling* encoder transits from the state $(m_1, m_2, \cdots, m_n)$ at time k-1 to the state $(m'_1, m'_2, \cdots, m'_n)$ at time k and generate the same encoder output.

Now let us consider the *reverse memory-labeling* encoder with the generator polynomial $g(x)$ in Fig. 8(b). With the state $(m_1, m_2, \cdots, m_n)$ at time k-1 and input b_k, the state at time k of the *reverse memory-labeling* encoder is given by

$$
S_n(k) = b_k + m_1 + \sum_{p=1}^{n-1} q_p m_{p+1} \overset{(a)}{=} b_k + b_k + \sum_{p=1}^{n-1} q_p m'_p + m'_n + \sum_{p=1}^{n-1} q_p m'_p = m'_n,
\tag{43}
$$

$$
S_p(k) = S_{p+1}(k) = m_{p+1} = m'_p,
\tag{44}
$$

where in the step (a) of (43) we have used Eq. (41).

The output of *reverse memory-labeling* encoder at time k is given by

$$
c(k) = m_{n+1} + \sum_{p=1}^{m-1} a_p m_{p+1} + m_1 = m'_m + \sum_{p=1}^{m-1} a_p m'_p + b_k + \sum_{p=1}^{n-1} q_p m'_p + m'_n,
\tag{45}
$$

where we have used Eq. (41) in the last step of calculation.

From (43-45), we can see that with input b_k the reverse memory-labeling encoder transits from the state $(m_1, m_2, \cdots, m_n)$ at time $k-1$ to the state $(m'_1, m'_2, \cdots, m'_n)$ and generates the same encoder output as the encoder with the generator polynomial $g(x)$.

This proves Theorem 3.

D. Proof of Theorem 5

To prove Theorem 5, let us first examine the backward decoding of a FBC code. At the encoder of a FBC code in Fig. 5, with input b_k, the state transits from $(m'_1, \cdots, m'_{n-1}, m'_n)$ at time $k-1$ to $(m_1, m_2, \cdots, m_n) = (c_k, m'_1, \cdots, m'_{n-1})$ at time k, where c_k is the encoder output. The state transition is shown in the Fig. 20, where a, d, $w=0$ or 1, $\bar{a} = 1 - a$, $\bar{d} = 1 - d$, and $\bar{w} = 1 - w$.
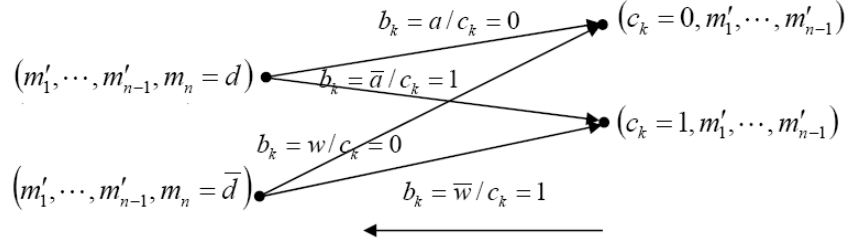
Fig. 20: The backward decoding trellis transition of a FBC code

Then we apply the BCJR backward decoding as follows,

(1) At time K, we have $\beta_K(0) = 1$ and $\beta_K(m) = 0$ for $m \neq 0$;

(2) At time K-1, we have

$\beta_{K-1}(m) = p_{c_K}(0)$ for $m = 0, 1$, and $\beta_{K-1}(m) = 0$ for $m \neq 0, 1$;

(3) At time K-2, we have

$\beta_{K-2}(m) = p_{c_{K-1}}(0)p_{c_K}(0)$, for $m = 0, 1, 2, 3$, and $\beta_{K-2}(m) = 0$, for $m \neq 0, 1, 2, 3$;

$\vdots$

(4) At time $K - v$, $0 \leq v \leq n$, we have

$\beta_{K-v}(m) = \prod_{i=0}^{v-1} p_{c_{K-i}}(0)$, for $m = 0, 1 \cdots, 2^v - 1$, and $\beta_{K-v}(m) = 0$, for $m \neq 0, 1 \cdots, 2^v - 1$;

$\vdots$

At time $K - t$, $t > n$, we have

$\beta_{K-t}(m) = \prod_{i=0}^{n-1} p_{c_{K-i}}(0)$, for all m.

From the above equation, we can see that $\beta_k(m)$ is the same for all states when $k \leq K - n$. Therefore, the backward decoding does not have any contribution in the probability calculation of the BCJR decoding. This proves that the BCJR forward decoding is exactly the same as the MAP decoding for the FBC codes.

E. Proof of Lemma 1

Let $S_i(k), i = 1, 2, \cdots, n$, and $S'_j(k), j = 1, 2, \cdots, n + l$, denote the memory of the i-th shift register of encoder C and the j-th shift register of encoder $\bar{C}$, generated by $g_{GC}(x)$ and $q_{GC}(x)$. According to Fig. 7a, in encoder C, $S_1(k + 1)$ is given by

$$S_1(k + 1) = b_{k+1} + \sum_{i=1}^{n} q_i S_i(k), \tag{46}$$

equivalently, we have the following equation

$$b_{k+1} = S_1(k+1) + \sum_{i=1}^{n} q_i S_i(k). \tag{47}$$

Let $q_0 = 1$ and $S_1(k+1) = S_0(k)$. Then (47) can be written as

$$b_{k+1} = \sum_{i=0}^{n} q_i S_i(k). \tag{48}$$

In encoder $\bar{C}$, the output b_{k+1} can be written as

$$b_{k+1} = c_{k+1} + \sum_{j=1}^{n+l-1} h_j S_j'(k)$$

$$= S_1'(k+1) + \sum_{j=1}^{n+l-1} h_j S_j'(k) + S_{n+l}'(k), \tag{49}$$

where we have used the relationship of $c_{k+1} = S_1'(k+1) + S_{n+l}'(k)$. Let $h_0 = h_{n+l} = 1$ and $S_1'(k+1) = S_0'(k)$, and we get

$$b_{k+1} = \sum_{j=0}^{n+l} h_j S_j'(k). \tag{50}$$

Since $h(x) = q(x)z(x) = q(x) + z_1 x q(x) + \cdots + z_{l-1} x^{l-1} q(x) + x^l q(x)$, we have

$$b_{k+1} = \sum_{i=0}^{n} q_i S_i'(k) + z_1 \sum_{i=0}^{n} q_i S_{i+1}'(k) + \cdots + z_{l-1} \sum_{i=0}^{n} q_i S_{i+l-1}'(k) + \sum_{i=0}^{n} q_i S_{i+l}'(k)$$

$$= \sum_{i=0}^{n} q_i \left\{ S_i'(k) + z_1 S_{i+1}'(k) + \cdots + z_{l-1} S_{i+l-1}'(k) + S_{i+l}'(k) \right\}. \tag{51}$$

Comparing (48) and (51), we can represent $S_i(k)$ by a linear combination of shift register memories of encoder $\bar{C}$

$$S_i(k) = S_i'(k) + z_1 S_{i+1}'(k) + z_2 S_{i+2}'(k) + \cdots + z_{l-1} S_{i+l-1}'(k) + S_{i+l}'(k). \tag{52}$$

Therefore, when tail bits of encoder $\bar{C}$ terminate it at the all-zero state, these tail bits will also terminate encoder C at the all-zero state.

This proves Lemma 1.

F. Proof of Lemma 2

With tail bits, both encoder $\bar{C}$ and its backward encoder begin with and end at the all-zero state, that is

$$\left(\overrightarrow{S_1'}(K+n+l), \overrightarrow{S_2'}(K+n+l), \cdots, \overrightarrow{S_{n+l}'}(K+n+l)\right) = (0, 0, \cdots, 0)$$

$$\left(\overleftarrow{S_1'}(K+n+l), \overleftarrow{S_2'}(K+n+l), \cdots, \overleftarrow{S_{n+l}'}(K+n+l)\right) = (0, 0, \cdots, 0). \qquad (53)$$

The state of encoder $\bar{C}$ and its backward encoder at time $K+n+l-1$ can be calculated as

$$\left(\overrightarrow{S_1'}(K+n+l-1), \overrightarrow{S_2'}(K+n+l-1), \cdots, \overrightarrow{S_{n+l-1}'}(K+n+l-1), \overrightarrow{S_{n+l}'}(K+n+l-1)\right)$$

$$= (0, 0, \cdots, 0, c_{K+n+l})$$

$$\left(\overleftarrow{S_1'}(K+n+l-1), \overleftarrow{S_2'}(K+n+l-1), \cdots, \overleftarrow{S_{n+l-1}'}(K+n+l-1), \overleftarrow{S_{n+l}'}(K+n+l-1)\right)$$

$$= (0, 0, \cdots, 0, c_{K+n+l}). \qquad (54)$$

This means that the encoder $\bar{C}$ and its backward encoder will arrive at the same state at time $K+n+l-1$. Let $\mathbf{u}' = \left(u_1', u_2', \cdots, u_{n+l}'\right)$ denote the state of encoder $\bar{C}$ at time $k-1$. Then its next state at time k is given by $\mathbf{u} = (u_1, u_2, \cdots, u_{n+l}) = \left(c_k + u_{n+l}', u_1', \cdots, u_{n+l-1}'\right)$. To prove that the encoder $\bar{C}$ and its backward encoder arrive at the same state any any time k, we only need to prove that the backward encoder will transit from state $\mathbf{u}$ at time k to state $\mathbf{u}'$ at time $k-1$. This can be proved in a similar way as the proof of Theorem 3 and we omit it here.

This proves Lemma 2.

G. Proof of Theorem 6

We consider a GC code generated by $g_{GC}(x) = \frac{a(x)}{q(x)}$. Its dual encoder for decoding is described by $q_{GC}(x) = 1 + \frac{h_1 x + \cdots + h_{n+l-1} x^{n+l-1}}{1 + x^{n+l}}$. We assume that the state of the dual encoder $\bar{C}$ transits from $\left(u_1', u_2', \cdots, u_{n+l}'\right)$ at time $k-1$ to $(u_1, u_2, \cdots, u_{n+l})$ at time k with input c_k. According to $q_{GC}(x)$, the output of the dual encoder $\bar{C}$ at time k can be written as

$$b_k = c_k + \sum_{j=1}^{n+l-1} h_j u_j'. \qquad (55)$$

For the bidirectional BCJR MAP algorithm, the probability that $b_k = w$ is given by

$$P_{b_k}(\omega) = P\{b_k = \omega|\vec{y}\} = \sum_{(u',u)=U(b_k=\omega)} \alpha_{k-1}(u')\gamma_k(u',u)\beta_k(u)$$

$$= \sum_{(u',u)=U(b_k=\omega)} \prod_{j=1}^{n+l-1} P_{\overrightarrow{S'}_j(k-1)}(u'_j) P(c_k) \prod_{i=2}^{n+l} P_{\overleftarrow{S'}_i(k)}(u_i)$$

$$= \sum_{(u',u)=U(b_k=\omega)} \prod_{j=1}^{n+l-1} P_{\overrightarrow{S'}_j(k-1)}(u'_j) \prod_{j=1}^{n+l-1} P_{\overleftarrow{S'}_j(k-1)}(u'_j) P(c_k)$$

$$= \sum_{c_k,u'_1,\cdots,u'_{n+l}, \sum_{j=1}^{n+l-1} h_j u'_j + c_k=\omega} \prod_{j=1}^{n+l-1} P_{S'_j(k-1)}(u'_j) P(c_k), \tag{56}$$

where $P_{S'_j(k-1)}(u'_j) = P_{\overrightarrow{S'}_j(k-1)}(u'_j) P_{\overleftarrow{S'}_j(k-1)}(u'_j)$. Let $L(b_k)$ denote the LLR of b_k. From (56), we can get

$$L(b_k) = L\left(\sum_{j=1}^{n+l-1} h_j S'_j(k-1) + c_k\right), \tag{57}$$

where $L\{S'_j(k-1)\} = \ln\frac{P_{S'_j(k-1)}(0)}{P_{S'_j(k-1)}(1)} = \overrightarrow{L}_{S'_j}(k-1) + \overleftarrow{L}_{S'_j}(k-1)$. Let $\hat{V}_j(k-1)$ denote the SSE of $S'_j(k-1)$, and we can get

$$\ln \hat{x}_{b_k} = \ln \hat{x}_{c_k} + \sum_{i=1}^{n+l-1} h_i \ln \hat{V}_i(k-1). \tag{58}$$

Comparing the shift register combined outputs of the dual encoder (16) and the outputs of the bidirectional BCJR MAP algorithm (58), we can see that they are exactly of the same.

REFERENCES

[1] P. Elias, "Coding for noisy channels," IRE Conv. Rec., pp. 4:37-47, 1955.

[2] A. Viterbi, "Error bounds for convolutional codes and an asymptotically optimum decoding algorithm," IEEE Trans. Inform. Theory, vol. 15, pp. 260-269, Apr. 1967.

[3] G. D. Forney, "The Viterbi algorithm", Proc. of IEEE, vol. 61, pp.268 - 278 , 1973.

[4] G. D. Forney, "Convolutional codes II: Maximum-likelihood decoding," Inform. Control, vol. 25, pp.222 - 250 , 1974.

[5] J. Hagenauer and P. Hoeher, "A Viterbi algorithm with soft-decision outputs and its applications," Proc. IEEE GLOBECOM, pp. 47.11-47.17, Dallas, TX, Nov 1989.

[6] L. Bahl, J. Cocke, F. Jelinek, and J. Raviv, "Optimal decoding of linear codes for minimizing symbol error rate," IEEE Transactions on Information Theory, vol. 20, no. 2, pp. 284 - 287, Mar 1974.

[7] J. Hagenauer, E. Offer, and L. Papke, "Iterative decoding of binary block and convolutional codes," IEEE Trans. Inf. Theory, vol. 42, no. 2, pp. 429-445, Mar. 1996.

[8] Y.Li, B. Vucetic, and Y. Sato, "Optimum soft-output detection for channels with intersymbol interference," IEEE Trans. Inf. Theory, vol. 41, no. 3 March 1995, pp. 704 - 713.

[9] Y. Li, M. S. Rahman, and B. Vucetic, SISO MAP decoding of rate-1 recursive convolutional codes: a revisit, Prof. ISIT 2012, MIT, Boston June 2012.